

Theory of near-field detection of core-gold nanoshells inside biosystems

M D'Acunto^{1, 2, 3*}, A Cricenti¹, M Luce¹, S Dinarelli¹

¹Istituto di Struttura della Materia, Consiglio Nazionale delle Ricerche, ISM-CNR, via Fosso del cavaliere, 100, I-00133, Roma, Italy

²Istituto di Scienza e Tecnologie dell'Informazione, Consiglio Nazionale delle Ricerche, ISTI-CNR, via Moruzzi 1, I-56124, Pisa, Italy

³NanoICT laboratory, Area della Ricerca CNR, Pisa, Italy

*Corresponding author: mario.dacunto@ism.cnr.it

Received 1 March 2015, www.cmmt.lv

Abstract

Metal nanoshells composed by a dielectric core with a thin gold layer are stimulating growing interests due to the unique optical, electric and magnetic properties exhibited by the local field enhancement near the metal – dielectric core interface due to strong local plasmon resonance and the high tunability of such resonance as a function of shape and core-material. These unique characteristics have found promising applications in a wide range of areas, such as biosensing, optical communication and medicine. In this paper, we developed a theoretical and numerical simulation based on a near-field approach to study the possibility to identify nanoshells inside mouse cells. Taking advantage from the characteristic near-infrared transparency window of many biological systems, i.e. the low light absorption coefficient of biological systems between 750-1100nm, we show the possibility to identify and detect 100-150nm diameter gold nanoshells inside the animal cells.

Keywords: Gold nanoshells, Mie theory, SNOM, animal cells, Near-infrared

1 Introduction. General requirements for sensing activity in biosystems

With recent advances in material synthesis and fabrication, metal nanoparticles have received considerable attention over the last decade [1-2]. Metallic nanoparticles when excited with an electromagnetic field, produce an intense absorption normally recognized as due to the collective oscillation of plasmon electrons on the particle surface. The resonance frequency is highly dependent on particle size, shape, material, and environment medium. Within the class of metallic nanoparticles, metal nanoshells stimulated the highest interest due to their remarkable optical properties [3-4]. Metal nanoshells are a type of nanoparticle composed of a non-metallic core and a metallic coating. Analogously to metal colloids, they show selective absorption peaks at specific wavelengths due to surface plasmon resonance. In addition, unlike bare metal colloids, the wavelengths, at which such resonance occurs can be tuned by changing the core radius or coating thickness or particle shape. Due to such relevant properties, metal nanoshell particles find one main application in medicine, where it is supposed that nanoshells with absorption peaks in the near-infrared can be attached to cancerous tumors and hence excited by a laser for heating them up and so killing the tumors cells [5-6]. The optical properties of such nanoshells in the near infrared (NIR) range is particularly important when they are used in biological systems because a certain range of wavelengths (700–1000nm), also called as *tissue transparency window*, is of special interest for in-depth cell investigations, thus making the NIR spectral range most convenient for a tailored instrumentation to look beneath the limits of visible outreach [7]. Even though NIR photons can travel farther than their shorter wavelength due to longer free path in the

matter, they become elastically scattered which makes direct microscopy impossible beyond the depth of several hundred microns. However, thanks to the higher transmittance rate, this spectral range allows for a number of image reconstruction techniques to re-build the original or close to original picture out of backscattered and dispersed non-ballistic photons.

In this paper we developed a theoretical and numerical simulation based on the near-field Mie theory to study the possibility to identify nanoshells inside animal cells. Taking advantage from the characteristic near-infrared transparency window of many biological systems, i.e. the low light absorption coefficient of biological systems between 750-1100nm, we were able to identify the 100-150nm diameter gold nanoshells inside the animal cells.

2 Far-to-near field quantitative Mie theory

In a system composed by a biological component like a cell and a population of metal nanoshell, the calculations of near field optical response must be reported accurately. The far-field response of a single nanoparticle with a diameter falling in the range 50-200nm can be calculated using the Mie theory [8]. Nevertheless, the near-field response require a supplemental work, stimulated recently by the rapid development in various fields, such as high spatial resolution of SNOM, single-molecule spectroscopy by surface-enhanced Raman scattering, nanodevices based on surface-plasmon photonic forces and quantum-optical processes in photonic crystals [9-12]. In all such fields, the calculation of the near field on ensembles of nanoparticles is a fundamental theoretical challenge. When the nanoparticles can be simplified to spheres, the analytical solution to the light scattering can

be obtained by extending the Mie theory. In a far-field treatment, one can consider at once to obtain a super-matrix, the so called T-matrix. T-matrix works well for far-field calculations of extinction-scattering-absorption spectra. However, for calculations of near field, this method fails due to irregular nanoparticles shape or induces mistakes due to nanoparticles aggregates of more than two particles. Because the entanglement of particles increases the size of the scattering matrix tremendous making difficult to manage accurate calculations with T-matrix. Another treatment is based on orders of scattering, which consist of a sum of simple scattering events from single particles in which the boundary conditions are considered in each scattering event. The core-shell particle is schematically described in figure 1(a) and the experimental system to detect a nanoshell inside a volume of dielectric constant ϵ_3 (in our case, the animal cell dielectric constant).

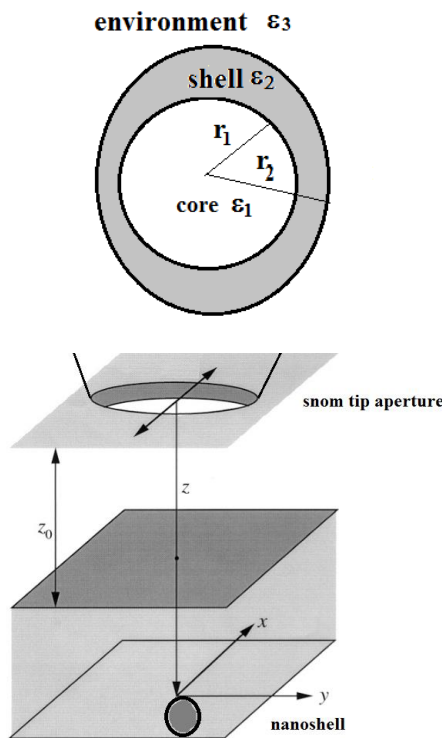


FIGURE 1 (upper) Schematic sketch of a nanoshell. The dielectric core of radius r_1 and the dielectric constant ϵ_1 forms the core region. The core is coated with a gold shell layer of thickness $r_2 - r_1$ and the dielectric function ϵ_2 and the shell forms the region 2. Finally, an embedding medium of dielectric constant ϵ_3 forms the third region, usually named the environment, in our paper, the environment is the air or the cell. (lower) The schematic sketch of the spatial dimensions of a SNOM aperture system. Note that the dimension of the SNOM aperture (normally 50nm diameter) is not in scale with the nanoshell dimension taken in consideration in this paper (100-150nm diameter).

For a satisfactory identification of nanoshells inside a biosystem using a NIR transparency window, we need to develop a near field treatment of gold nanoshell. Following the approach of Stratton, we solve the Maxwell's equations for incident fields as time-harmonic, with an $\exp(-i\omega t)$ dependence so that a vector basis function formalism can be used [13-15]. In a linear, isotropic medium, with no external sources and no divergence of the electric field, the general

diffraction equation takes on the form of the vector Helmholtz equation

$$\nabla \times \nabla \times \mathbf{E} - \omega^2 \mu \epsilon \mathbf{E} = 0 \quad (1)$$

where ω is the angular frequency and ϵ is the dielectric function and μ the magnetic permeability. This equation describes the propagation of scalar waves in a medium. Introducing a scalar generating function ψ , eq. 1 can be written as

$$\nabla^2 \psi(\mathbf{r}, t) + k^2 \psi(\mathbf{r}, t) = 0 \quad (2)$$

The e.m. fields of the incident wave, scattered wave, and the wave inside the particle can in general, be written as a series expansion of the spherical harmonics basis vectors (\mathbf{M} , \mathbf{N} , \mathbf{L}) [13-15]. \mathbf{M} , \mathbf{N} , and \mathbf{L} can be constructed as follows

$$\mathbf{M} = \nabla \times (\mathbf{c}\psi), \quad \mathbf{N} = (\nabla \times \mathbf{M}) / k, \quad \mathbf{L} = \nabla \psi \quad (3)$$

where \mathbf{c} is an arbitrarily constant vector and $k^2 = \omega^2 \epsilon \mu$ is the wave-number of the electromagnetic wave. Due to the required orthogonality and completeness of such basis, we can write the electric or magnetic field as a series of the spherical vector basis functions

$$\mathbf{E} = \sum_{mn} \{ a_{mn} \mathbf{M}_{mn} + b_{mn} \mathbf{N}_{mn} + c_{mn} \mathbf{L}_{mn} \} \quad (4)$$

The field is completely defined by the coefficients (a_{mn} , b_{mn} , c_{mn}), and if the divergence is assumed to be zero, the coefficients c_{mn} can be considered zero, so that the contribution to the field is given only by \mathbf{M} and \mathbf{N} .

For light scattering from a nanoshell, the electromagnetic fields must satisfy Maxwell's boundary conditions at each layer boundary of the interfaces sketched in figure 1. At the interface between penetrable materials such as dielectrics and metals with finite conductivity, the tangent components of the electromagnetic fields are continuous, i.e. the fields are subject to the boundary conditions:

$$\hat{\mathbf{n}}(s) \times \mathbf{E}_{s^-} = \hat{\mathbf{n}}(s) \times \mathbf{E}_{s^+} \quad \text{and}$$

$\hat{\mathbf{n}}(s) \times \mathbf{H}_{s^-} = \hat{\mathbf{n}}(s) \times \mathbf{H}_{s^+}$, where s is a point on the surface and s^- and s^+ are the points just inside or out the sphere, respectively.

For a spherical nanoshell with the plane wave incident field defined in equation 2, the electric fields can be expressed as a series of the vector harmonics in the 3 regions as

$$\mathbf{E}_1 = \sum_{n=1}^{\infty} \left\{ a_{\pm 1n}^{(1)j} \mathbf{M}_{\pm 1n}^{(1)j} + b_{\pm 1n}^{(1)j} \mathbf{N}_{\pm 1n}^{(1)j} \right\}, \quad (5a)$$

$$\mathbf{E}_2 = \sum_{n=1}^{\infty} \left\{ a_{\pm 1n}^{(2)j} \mathbf{M}_{\pm 1n}^{(2)j} + b_{\pm 1n}^{(2)j} \mathbf{N}_{\pm 1n}^{(2)j} + a_{\pm 1n}^{(2)b} \mathbf{M}_{\pm 1n}^{(2)b} + b_{\pm 1n}^{(2)b} \mathbf{N}_{\pm 1n}^{(2)b} \right\}, \quad (5b)$$

$$\mathbf{E}_3 = \sum_{n=1}^{\infty} \left\{ a_{\pm 1n}^{(3)b} \mathbf{M}_{\pm 1n}^{(3)b} + b_{\pm 1n}^{(3)b} \mathbf{N}_{\pm 1n}^{(3)b} \right\}. \quad (5c)$$

and analogous expressions are obtained for the magnetic fields $\mathbf{H}_i = -i \sqrt{\epsilon_i / \mu_i} \mathbf{E}_i$. In the eqs. (5), the superscripts represent the regions and the types of the scattering coefficients. The region that includes the core (region 1) has only radial contributions from the spherical Bessel functions (denoted by the superscript j), while regions that are not bounded as the environment (region 3) contain only the Hankel functions of the first kind (h). Finally, region 2 containing the gold shell presents contributions from both types of functions. Indeed, it should be noted that the scalar Helmholtz equation presents solutions that in spherical-polar coordinates are as follows

$$\psi_{nm}(r, \theta, \varphi) \cong z_n(kr) P_n^m(\cos \theta) e^{im\varphi}, \quad (6)$$

where $z_n(kr)$ denotes either the spherical Bessel functions $j_n(kr)$ or the spherical Hankel functions of the first kind, $h_n(kr)$, and the $P_n^m(\cos \theta)$ are the associated Legendre functions. It should be pointed out that the Bessel functions are regular at the origin, whereas the spherical Hankel functions diverge at the near the origin. As a consequence, a region including the core can only present spherical Bessel functions in its expression for the field. While, in contrast, a region not including the origin, as the shell, should have contributions from both such functions. Solving the eqs. (5) for the electric field and the corresponding expression for the magnetic fields we can obtain the fields everywhere. All

$$a_n = \frac{\psi_n(y) [\psi_n'(m_2 y) - A_n \chi_n'(m_2 y)] - m_2 \psi_n'(y) [\psi_n(m_2 y) - A_n \chi_n(m_2 y)]}{\xi_n(y) [\psi_n'(m_2 y) - A_n \chi_n'(m_2 y)] - m_2 \xi_n'(y) [\psi_n(m_2 y) - A_n \chi_n(m_2 y)]}, \quad (8a)$$

$$b_n = \frac{m_2 \psi_n(y) [\psi_n'(m_2 y) - B_n \chi_n'(m_2 y)] - \psi_n'(y) [\psi_n(m_2 y) - B_n \chi_n(m_2 y)]}{m_2 \xi_n(y) [\psi_n'(m_2 y) - B_n \chi_n'(m_2 y)] - \xi_n'(y) [\psi_n(m_2 y) - B_n \chi_n(m_2 y)]}, \quad (8b)$$

$$\text{with } A_n = \frac{m_2 \psi_n(m_2 y) \psi_n'(m_2 x) - m_1 \psi_n'(m_2 x) \psi_n(m_1 x)}{m_2 \chi_n(m_2 x) \psi_n'(m_1 x) - m_1 \chi_n'(m_2 x) \psi_n(m_1 x)}$$

$$\text{and } B_n = \frac{m_2 \psi_n(m_1 x) \psi_n'(m_2 x) - m_1 \psi_n'(m_2 x) \psi_n(m_1 x)}{m_2 \chi_n(m_2 x) \psi_n'(m_1 x) - m_1 \chi_n'(m_1 x) \psi_n(m_2 x)},$$

where $x = kr_1 = 2\pi N r_1 / \lambda$ and $y = kr_2 = 2\pi N r_2 / \lambda$ are the size parameters of the core and the shell respectively, and m_1 and m_2 is the relative refractive index of the core and the shell to that of environment medium. ψ_n , χ_n and ξ_n are the Riccati-Bessel functions, and the primes indicate differentiation with respect to the argument [17]. If the limit of small particles is taken in consideration, the Riccati-Bessel functions can be expanded in power series, and while the denominator of b_n will never vanish for any n , the denominator of a_n will vanish as $x \rightarrow 0$, and $y \rightarrow 0$, $m_2 = i(n+1/n)^{1/2}$, with $n=1,2,\dots$. For example for a dipole $m_2 = i\sqrt{2}$, that requires a negative refractive index, condition satisfied by a metallic particles. The presence of the core provides a shift that depends on $f = (r_1/r_2)^3$, i.e. the volume fraction of the core and the total volume, and the dielectric constant of both core and shell. We simulated red-shifts for several core materials, such as SiO₂, TiO₂ and BaTiO₃, for nanoshell particles with diameters falling in the range 100-150nm (with core-shell ratio of 75%), the most relevant shift

the numerical results were obtained writing a specific code based on Matlab® language and using the boundary element method (BEM) [16].

The far-field scattering properties, absorption and extinction cross-sections emerging from the nanoshell can be determined determining the coefficients a and b in eq. (5). In terms of such coefficients, and analogously to the standard Mie theory [8], we obtain

$$\sigma_{sca} = \frac{2\pi}{k^2} \sum_{n=1}^{\infty} (2n+1) \left(|a_{1n}^{(3)h}|^2 + |b_{1n}^{(3)h}|^2 \right), \quad (7a)$$

$$\sigma_{ext} = -\frac{2\pi}{k^2} \sum_{n=1}^{\infty} (2n+1) \text{Im} \left(a_{1n}^{(3)h} + b_{1n}^{(3)h} \right), \quad (7b)$$

$$\sigma_{abs} = \sigma_{ext} - \sigma_{sca}. \quad (7c)$$

In Mie theory the electric and magnetic fields are expressed as infinite sums over the vector spherical harmonics, eqs. (5a-c), and the harmonics for the scattered fields are weighted by the coefficients a_n and b_n , eqs. (7a-c). The vector spherical harmonics represent normal modes of the nanoshell, with the two modes for each n corresponding to transverse magnetic and transverse electric modes, where there is no radial electric and magnetic fields respectively. For the case of a nanoshell of core radius r_1 and total radius r_2 , the coefficients a and b are given as follows [8, 15]:

towards NIR was observed for the BaTiO₃ core based nanoshells, [16]. Second harmonic generation for a BaTiO₃ core gold nanoshell has been recently described in [18]

In far-field conditions, the scattering contributions generally dominate with the respect the absorption contributions, making very difficult to detect nanoshells. In the local near field around the nanoshell, the absorption efficiency can be enhanced by the coupling with the plasmon oscillations. The Mie theory developed and utilized for the far field quantification of the plasmon-e.m. coupling can be used for the near field case as a limiting case.

3 Numerical simulation of the optical response of gold nanoshells as observed using an aperture SNOM

Near-field enhancement due to plasmonic coupling of the nanoshell with external e.m. field should produces measurable effects, particularly, when the evanescent wave is not absorbed by the biological system. In practice, if nanoshells are located just under a short depth inside the biological system we could collect signals identifying absorbing objects with the dimensions of the nanoshell particles. To confirm such prevision, we have simulated the optical signal detected by an aperture SNOM operating in air in collection mode with different illumination wavelengths ranging from visible to near infrared. The samples

used for the experimental testing are animal cells, interacting with gold nanoshells with dielectric core (SiO_2 , BaTiO_3). Preparation of cell samples are described elsewhere [19], while the interest in using BaTiO_3 as the dielectric core of the sample is due essentially to the relevant shift towards near infrared shown by nanoshells with 100nm and 20nm dimension for core and shell respectively [16].

The SNOM is considered to be used in reflection mode measurements with aperture tips of nearly 50nm diameter. The extinction signal of cell samples has been detected in reflection acquisition mode: the sample can be illuminated

on top by an external source, laser, with different wavelengths λ , ($\lambda=488\text{nm}$, 632nm , 780nm , 980nm were used), an optical fiber was used for the detection of the reflected signals. If the nanoshell is located just under the cell cytoskeleton, and the evanescent signal produced by the nanoshell is not absorbed by the cell due to the transparency window, then it should be possible to locate the nanoshell inside the cell, see figure 2, where the (a) image corresponds to the topography of a cell recorded with a SNOM system. Fig. 2 (b) represents the line-trace along the white line in (a) (full line) together with the contour simulation (dashed line) and the nanoparticles distribution (small circles).

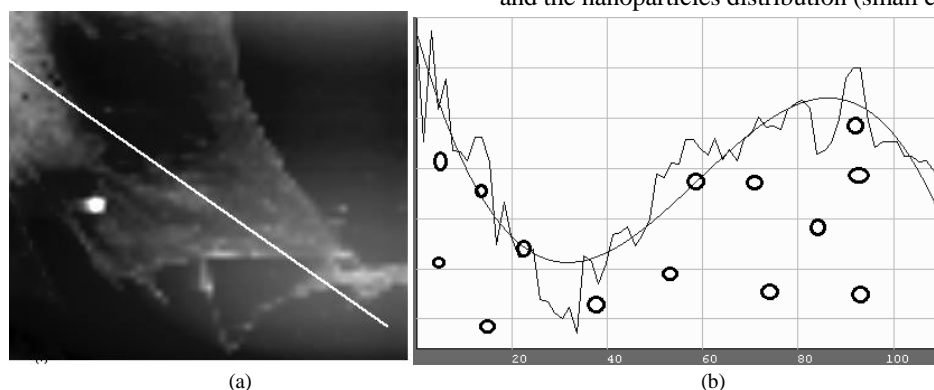


FIGURE 2 (a) Topographic image of a cell recorded with a SNOM, and (b) schematic sketch of the distribution of nanoshells (back circles) inside a cell

In figure 3, we report the results of a Finite Difference Time Domain (FDTD) simulation of a single nanoshell obtained simulating a SNOM operating in collection mode with a 780nm wavelength laser light with nanoshell dis-

persed inside an animal cell (for instance, we have considered dielectric constant of the h9c2 mouse type cell, [20]). The fields simulated and the Poynting vector are calculated along the z-direction, with the origin fixed at the SNOM aperture.

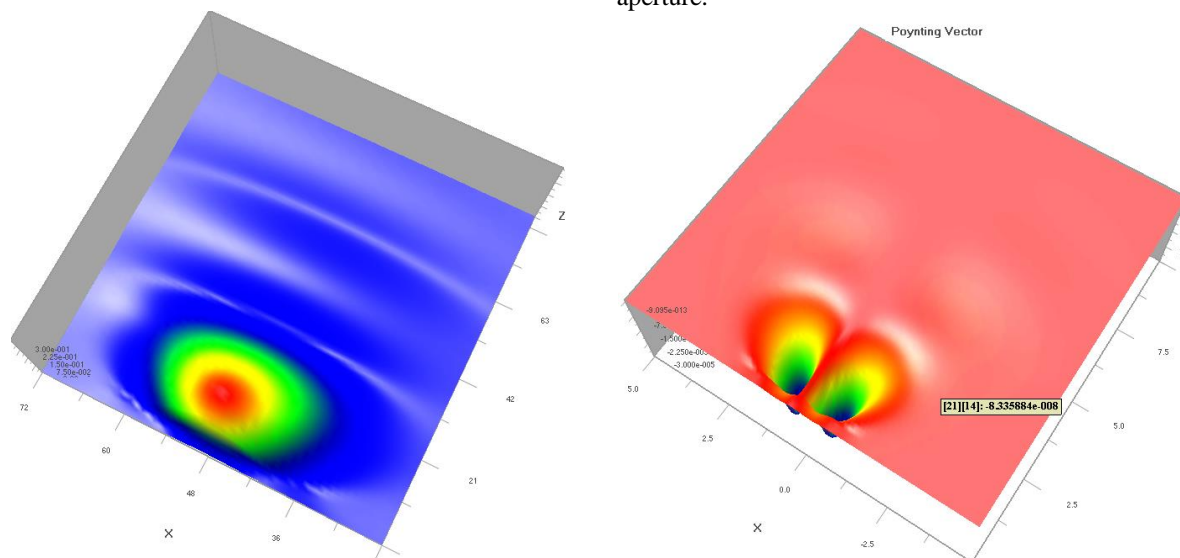


FIGURE 3 (upper) FDTD simulation of a gold nanoshell recorded with the SNOM operating in collection mode. The gold nanoshell can be represented as point-like absorption sources due to near-field enhancement due to plasmonic coupling of the nanoshell with external e.m. (a) E_z component of the extinction fields due to confined plasmonic nanoshelle behavior; (lower) correspondent Poynting vector

The gold nanoshells as observed by a SNOM in reflection mode are denoted by *point-like absorption sources*. Point-like absorption source presents dimension very close to nanoparticle falling in the range 120-150nm diameters, so that the identification of such points with the gold nanoparticles is immediate. The isolated point-like

sources can be immediately identified as the core-shell nanoparticles. The electric field distribution along the z-direction of a particle located at \mathbf{a} and collected at the SNOM tip aperture, as represented in figure 3(a), is approximately given by the expression [21]:

$$E_z(\mathbf{r}, t) \equiv E_0(\mathbf{p} \cdot \mathbf{n})(\mathbf{n} \cdot \mathbf{e}_a) \frac{\cos(kr_a - \omega t)}{\sqrt{r_a}} \exp(-r_a/l), \quad (9)$$

where \mathbf{E}_0 and \mathbf{p} are the electric field amplitude and the polarization direction of the illuminating light, respectively; $r_a = |\mathbf{r}_a| = |\mathbf{r} - \mathbf{a}|$ is the magnitude of the separation vector with $\mathbf{e}_a = \mathbf{r}_a/r_a$ being the unit vector. The terms $\mathbf{p} \cdot \mathbf{n}$ and $\mathbf{n} \cdot \mathbf{e}_a$ describe the role of the polarization on the efficiency of near field plasmon-e.m. coupled excitation, being \mathbf{n} the normal vector to the probe (recognized as the maximum dipole radiation) and the cosine angular distribution of the radiation, respectively. The two factors k and l represent the propagation constant and the length of the nanoparticles plasmonic field, respectively. The detected SNOM signal is formed by the complex light scattering processes between the tip and the sample, mixing different field components. Thus, electromagnetic field collected near the probe cannot be simply linked to a specific component of the unperturbed electromagnetic field distribution.

To exhibit the relative absorption and scattering ability of the nanoshells, the cross sections for absorption and scattering can be defined as $\sigma_{abs} = W_{abs}/I_{inc}$ and $\sigma_{scat} = W_{scat}/I_{inc}$ respectively, while the efficiencies are defined as $Q_{abs} = \sigma_{abs}/A$ and $Q_{scat} = \sigma_{scat}/A$, for the absorption and the scattering processes, respectively. Here, $I_{inc} = (1/2)\epsilon_0 c E^2$ represents the intensity of the incident wave, $A = \pi r^2$ is the particle cross-section projected onto a plane perpendicular to the incident wave, and r is the total radius on the nanosphere. Finally, the absorption and scattering energy $W_{abs/scat}$ are defined respectively as

$$W_{abs} = \frac{1}{2} \text{Re} \left[\iint \left(\mathbf{E}_{tot} \times \mathbf{H}_{tot}^* \right) \cdot \mathbf{n} ds \right] \text{ and}$$

$$W_{scat} = \frac{1}{2} \text{Re} \left[\iint \left(\mathbf{E}_{scat} \times \mathbf{H}_{scat}^* \right) \cdot \mathbf{n} ds \right]. \quad (10)$$

In far field, we can insert the components fields as given by the eqs. 5a and 5b, inside eqs (10), and integrating on all a solid angle; on the contrary, in near field, if we consider a finite dimension of tip aperture, we have that scattered and absorbed intensities are proportional to the solid angle.

In addition, if we consider a near field solution of electric and magnetic fields and the field enhancement in z -direction in proximity of the SNOM probe tip, under some specific condition we can observe intense enhanced absorption, The E_z components under the SNOM tip could be about 10 times larger if compared to the in-plane components, so, it is

References

- [1] Kelly K L, Coronado E, Zhao L L, G C Schatz G C 2003 *J. Phys. Chem. B* **107** 668
- [2] Myroshnychenko V, Rodríguez-Fernández J, Pastoriza-Santos I, Funston A M, Novo C, Mulvaney P, Liz-Marzán L M, García de Abajo F J 2008 *Chem. Soc. Rev.* **37** 1792
- [3] Jackson J B, Westcott S L, Hirsch L R, West J L, Halas N J, 2003 *Appl. Phys. Lett.* **82** 257
- [4] Hirsch L R, Gobin A M, Lowery A R, Tam F, Drezek R A, Halas N J, West J L 2006 *Ann. Biomed. Eng.* **34** 15
- [5] Lin A W H, Halas N J, Drezek R A 2005 *J. Biomed Opt.* **10** 064301
- [6] Liu C, Mi C C 2008 *IEEE Transactions of Nanobioscience* **7** 206

reasonable to suppose that when the probe signal displays a point-like absorption peaks, this can be identified with a nanoshell [22]. This is because the field enhancement caused by the local surface plasmon resonance mainly focuses on the metal-dielectric interface (and decays exponentially) is not absorbed by the biological tissue due to the transparency window. In figure 4, we have calculated the absorption (continue line) and the scattering coefficients (dashed line) for a nanoshell with a varying gold layer in the range 0-100nm, with a BaTiO₃ core dimension fixed at 100nm. Our nanoparticles should have a nominal gold layer of 20-40nm, i.e., in the region where the absorption is significantly higher with respect to scattering mechanisms.

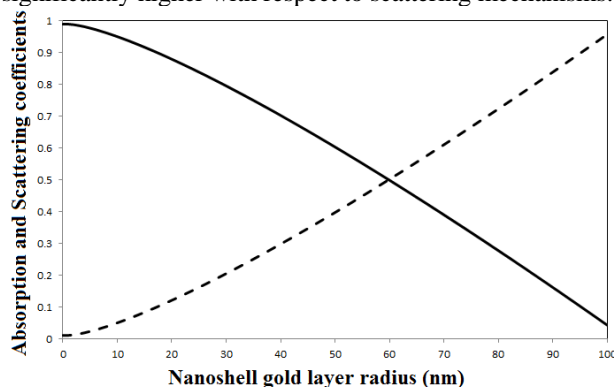


FIGURE 4 Absorption and scattering efficiency coefficients as a function of gold nanoshell layer dimension. The BaTiO₃ core was fixed at 100nm

Finally, one open problem is represented by the optical response of gold nanoparticles clusters that could present the enlarged absorption regions. The interpretation of nanoshell cluster signals that could be source of controversial interpretation require supplementary theoretical and numerical tools [23].

5 Conclusions

In this paper, a theoretical and numerical approach has been developed to support the possibility to use an aperture SNOM (aperture nearly 50nm diameter) to identify 100-150nm diameter gold nanoshells inside animal cells. The results confirm that SNOM is able to identify nanoshells located inside the upper cell layers.

Acknowledgments

The authors would like to acknowledge the contribution of the COST Action MP1302 Nanospectroscopy.

- [7] König K 2000 *J. Microscopy* **200** 83
- [8] Mie G 1908 *Ann. Phys. (Leipzig)* **25** 377
- [9] Zavelani-Rossi M, Celebrano M, Biagioni P, D. Polli D, Finazzi M, Duò L, Cerullo G, Labardi M, Allegrini M, Grand J, Adam P M 2008 *Applied Physics Letters* **92** 093119
- [10] Fan P, Chettair U K, Cao L, Afshinmanesh F, Engheta N, Brongersma M L 2012 *Nature Photonics* **6** 380
- [11] Feng J, Siu V C, Roelke A, Metha V, Rhieu S Y, Palmore G T R, Pacifici D 2012 *Nano Letters* **12** 602
- [12] Chen Y F, Serey X, Sarkar R, Chen P, Erickson D 2012 *Nano Letters* **12** 1633

- [13] Stratton J A 1941 *Electromagnetic Theory* McGraw-Hill:New York
- [14] Sarkar D, Halas N J 1997 *Physical Review E* **56** 1102
- [15] Le D SURE Project, Spectroscopic Characterization of Silica-Gold Nanoshells, available at <http://www.cmmu.ucl.ac.uk/~mdl/cam/Mie/nanoshells.pdf>
- [16] D'Acunto M, Moroni D, Salvetti O 2012 *Advances in Optical Technologies*
- [17] Gradshteyn I S, Ryzhik I M 2007 *Table of Integrals, Series and Products* Seventh Edition, A. Jeffrey and D. Zwillinger eds.
- [18] Farrokh Takin E, Ciofani G, Puleo G, de Vito G, Filippeschi C, Mazzolai B, Piazza V, Mattoli V 2013 *International Journal of Nanomedicine* **8** 2319
- [19] Cricenti A, Marocchi V, Generosi R, Luce M, Perfetti P, Vobornik D, Margaritondo G, Talley D, Thielen P, Sanghera J S, Aggarwal I D, Miller J K, Tolk N H, Piston D W 2004 *Journal of Alloys and Compounds* **362** 21
- [20] Stacey M W, Sabuncu A C, Beskok A 2015 *Biochim. Biophys. Acta* **1840**(1-12)
- [21] Dvorák P, Neuman T, Brínek L, Šamoril T, Kalousek R, Dub P, Varga P, Šíkola T 2013 *NanoLetters* **13** 2558
- [22] Nedyalkov N N, Dikovska A, Dimitrov I, Nikov R, Atanasov P A, Toshkova R A, Gardeva E G, Yossifova L S, Alexandrova M T 2012 *Quantum Electronics* **42** 1123
- [23] Girard C 2005 *Report on Progress of Physics* **68** 1883

Authors	
	<p>Antonio Cricenti, 28/05/1959, Monterosso Calabro (I)</p> <p>Current position, grades: Research Director, National Research Council University studies: PhD in Physics Scientific interest: Surface Physics, Semiconductors, Biological cells Publications: 220 international peer reviewed publications Experience: Ultra-high-vacuum, scanning probe microscopy, clean semiconductor surfaces, biological material</p>
	<p>Mario D'Acunto, 20/08/1966, Minturno (I)</p> <p>Current position, grades: Researcher, National Research Council University studies: PhD in Surface Mechanics Scientific interest: Surface Physics, Nanotribology, Soft matter Publications: 100 international peer reviewed publications Experience: scanning probe microscopy, friction and wear, sensors</p>
	<p>Marco Luce, 26/05/1967, Roma (I)</p> <p>Current position, grades: Electronic engineering, National Research Council University studies: Electronic degree Scientific interest: Surface Physics, Semiconductors, Biological cells Publications: 42 international peer reviewed publications Experience: Ultra-high-vacuum, scanning probe microscopy, clean semiconductor surfaces, biological material</p>
	<p>Simone Dinarelli, 26/05/1984, Roma (I)</p> <p>Current position, grades: post-doc of the Institute of Structure of Matter, National Research Council, Rome University studies: PhD in biochemistry, University of Rome "La Sapienza" Scientific interest: He is a specialist in the field of SNOM and AFM in material science and biology.</p>